Impact of 3D printing materials on mircoalga *Chlorella vulgaris*

Victor Pozzobon[1] ✉, **Franco Otaola**[1], **Clarisse Arnoudts**[1], **and Jules Lagirarde**[1]

[1]LGPM, CentraleSupélec, Université Paris-Saclay, SFR Condorcet FR CNRS 3417, Centre Européen de Biotechnologie et de Bioéconomie (CEBB), 3 rue des Rouges Terres 51110 Pomacle, France

3D printing represents a key enabling technology in designing photobioreactors. It allows rapid prototyping of complex geometries at an affordable price. Yet, no study dealt with the biocompatibility of 3D printing material with microalgae. Thus microalga *Chlorella vulgaris* was cultivated in contact with different 3D printing materials (Acrylonitrile Butadiene Styren - ABS, PolyCarbonate Blend - PC-Blend , PolyLactic Acid - PLA, and acrylate methacrylate resin). Cell status was analyzed using flow cytometry, fluorometry, and pigment profiling. Results revealed that acrylate methacrylate resin material inhibits growth and decreases photosynthetic apparatus functioning. ABS, PC-Blend, and PLA led to nominal perfromances. Nevertheless, PLA was the only material that did not induce an early onset of intracellular reactive oxygen species. Therefore, resin can be ruled out as photobioreactor material, ABS and PC-Blend could be used after a curation period, and PLA induces no detectable perturbations by the means used in this study.

Graphical abstract

Microalgae | 3D printing | Oxidative stress | Flow cytometry | Pigment
Correspondence: *victor.pozzobon@centralesupelec.fr*

1. Introduction

Photosynthetically cultivated microalgae are regarded as small biological factories capable of producing many molecules with applications ranging from food and feed to advanced compounds used in the cosmetic and pharmaceutical industries (1, 2). Still, before they realize the full extent of their promises, their production cost has to be considerably lowered. Photobioreactor design is key to this goal. Indeed, numerous studies have highlighted that the combination of geometry and light delivery could lever high-density and high-quality cultures (3–6). Nevertheless, the best way to combine illumination and geometry, if any, has yet to be unanimously acknowledged (7). Instead of finding a universal optimum for light and geometry combination, it is far more likely that each strain-end product couple will have its own. With this in mind, one can expect long and complex explorations of hand-tailored photobioreactor designs. Still, two tools come to assist scholars and engineers. First, computational fluid dynamics allow fluid flow and illumination reproduction within a numerical photobioreactor design (8). This way, it is possible to quickly assess for shear stress (9) and light patterns (10–12), without even going to physical design process. Therefore, it allows the discard of unpromising designs at an early stage of the conception process. Second, 3D printing allows a fast transition from a digital design to a physical object at an affordable price, enabling what is commonly known as rapid prototyping (13). This approach is a potent tool to confirm or discard designs at an affordable price before their fabrication in a more resistant material, which generally requires more expensive and slower fabrication technologies. Finally, 3D printing offers wider geometrical freedom than classic technologies, enabling conceiving reactors with advanced geometries.

Despite this undeniable potential for microalgal biotechnology, articles combining 3D printing and microalgae are still few in the literature. Even more surprising, none explicitly dealt with the biocompatibility of 3D printing material with microalgae, despite the fact that it represents a pivotal prerequisite to their use. Among the few emerging articles, nascent categories arise. The closest to the envisioned application in this article is the use of 3D printing to design parts intended for long-term use in the marine environment (aquaculture farms, ships, marine sensors, ...) (14). In this context, the ability of 3D printing material to repel biofouling is of interest, which represents an adverse focus with respect to the current work. Nevertheless, the authors showed that all the tested materials (comparable to the ones used hereinafter) were covered with biofilm (86 % or more) in twelve weeks. Furthermore, they examined the biofilm taxonomy and discovered that early colonization was led by cyanobacteria, replaced in steady state by microalgae (30 to 60 % of the total flora), supporting the idea of a possible long-term association of 3D printing materials and microalgae.

A second category of 3D printing material/microalgae interaction is the application of 3D printing to design parts (15), sensors (16), or modules for microalgae-related processes (17). For example, Syed *et al.* designed an hydrocyclone allowing to pre-concentrate a microalgae culture (from 0.045 MCell/mL to 3.2 MCell/mL, *i.e.*, 7.13 concentration factor) (17). In their work, the authors used Visijet M3 Crystal 3D printing material as it is medical grade, claiming biocompat-

ibility with blood cells. With such a material, the authors aimed at minimizing the effect of the 3D printing material on the cells, yet, without confirming this biologically. Nevertheless, given the short contact time between the cells and the material (below 1 minute), they could have resorted to other materials, as Visijet M3 Crystal is about ten times more expensive than classical polylactic acid. In addition to the cost of the material itself, the 3D printing technology used for this fabrication was multi-jet printing. This professional technology is not available to the general public and is far more expensive. Another study examined how 3D printed structures could help manage biofilm in photobioreactors (15). The authors showed that adequately shaped and sized structures (*i.e.*, 10 mm spheres) could significantly reduce biofilm formation by managing bubble bursting and yield almost doubled biomass and lipid productivities. Nevertheless, they did not investigate nor mention a potential effect of prolonged contact between microalgae and 3D printing material.

Moving away from the focus of this work, another category of application combining microalgae and 3D printing is food 3D printing (18, 19). Authors have investigated the feasibility and relevance of such a combination using robocasting technology, where a slurry is deposed layer by layer to create the object using a syringe as the extruder of the system. They conclude that microalgae inclusion (up to 4 % in mass) increased the pressure required to extrude the dough but does not alter the final results in terms of shape. They also showed that it was possible to co-extrude microalgae-enriched dough within classical dough. This way, microalgae supplementation, which hinders the product's appeal by making it darker, can be hidden within regular dough, creating a cookie that is both microalgae-enriched and regular looking.

Finally, one is to mention that high density (45 % in volume in water or oil) *Chlorella* paste (from dried microalgae) was also demonstrated to be 3D printable (20), especially when mixed with hexane and oil. However, the scope of application for this process remains to be deciphered.

All in all, there is, to the authors knowledge, no study dedicated to the impact of 3D printing materials on microalgae. Nevertheless, by widening the scope, one has to mention a study led on zebrafish which concluded to the toxicity (lower hatching and survival rates, higher occurrence of developmental abnormalities) of common 3D printing materials (21). Nevertheless, zebrafish are complex organisms, higher placed in the trophic chain, and undoubtedly too different from microalgae to translate any conclusion. Therefore, this work aims at filling this gap in the literature. To do so, *Chlorella vulgaris* was cultivated in contact with four different 3D printing materials: Acrylonitrile Butadiene Styren (ABS), PolyCarbonate Blend (PC-Blend), PolyLactic acid (PLA), and acrylate methacrylate resin. The three first correspond to the affordable and widespread Fused Filament Fabrication 3D printing technique. The last one is used for stereolithographic 3D printing by photopolymerization of a resin. Among the notable differences between the two techniques, the key one in the context of photobioreactor prototyping is the water tightness of the material under pressure. While both techniques can produce watertight objects, only the stereolithographic technique allows the parts to handle high water pressure, as its results do not feature any microporosity. This might be convenient if one wants to design a long tubular photobioreactor with a high pressure drop between the inlet and the outlet. Still, the stereolithographic techniques may suffer a potential drawback. Indeed, as they use photosensitive resins and as photobioreactors are constantly exposed to light, this might reduce the lifetime of designed parts.

Chlorella vulgaris was chosen as the model strain for two reasons. First, *Chlorellae* make a fast-growing and ubiquitous genus often used for ecotoxicological studies (22, 23). Second, from a biotechnological point of view, *Chlorella vulgaris* is commonly encountered in industrial and scientific communities, approved as food and feed by (EFSA - Ares (2022) 1668627 - and US FDA - GRN 00396 -), and features a sizable potential (24). Among the potential applications, scholars investigated bioenergy (25, 26), phycoremediation (27), biofertilisation (28), protein production (29, 30), ...

The cultures were led in shake flasks over six days until the entry of the culture in the stationary phase. For each material, the cells were put in contact with one, two, or three 10 mm 3D printed cubes of the selected materials (biological duplicate, with positive and negative control). This protocol was retained to assess for a potential dose-response mechanism. Cell proliferation was monitored daily by means of optical density recording. In addition, cell status (morphology, chlorophyll fluorescence, and intracellular reactive oxygen species) was also followed daily using a flow cytometer. At the end of the runs, microalgae photosynthetic apparatus status was qualified by fluorometric assays, and their pigment content was also quantified. Finally, submerged cubes were recovered and observed using a microscope to check for microalgae colonization of the structure or alteration of the material.

2. Materials and methods

2 1. Strain and culture medium

The *Chlorella vulgaris* strain (CV 211-11b) was obtained from Sammlung von Algenkulturen (SAG) Culture Collection, Germany. B3N medium (autoclaved) (31) was used throughout this study. Before entering the test phases, cells were subcultured in this medium for more than five generations. This medium was chosen as, from our group experience, it allows flourishing cultures of *Chlorella vulgaris*.

2 2. Cultivation and tested conditions

Tests were conducted in shake flasks (250 mL, 50 mL medium, 100 rpm) under continuous moderate light (50 µmolPhotonPAR/m^2/s) for six days. Moderate illumination was chosen to allow high pigment expression, therefore magnifying potential discrepancies between the tested configurations. Furthermore, preliminary tests within our device showed that, under nominal conditions, six days were sufficient for the culture to enter the early stationary phase. Finally, cultures were not supplemented in carbon dioxide, and temperature was kept within a 22-24 °C range.

For each material (ABS, PC-Blend, PLA, and resin), a set of 10 mm side cubes was fabricated out of a single batch of raw material. ABS (Raide3D^{TM} Premium) and PLA (3D Printz Ltd.) were printed with Creality CR-10 Max 3D printer (slicer - PrusaSlicer 2.6.0). PC-Blend (Prusament PC Blend Natural) was printed with Prusa MK3 printer (slicer - PrusaSlicer 2.6.0). Cubes made of resin (3DM-TOUGH) were printed with Prusa SL1S printer (slicer - PrusaSlicer 2.6.0). Furthermore, these last cubes were postprocessed by UV light exposure, as recommended by the manufacturer, and the study of Oskui *et al.*, who showed significantly lower toxicity of the material after curation (21). Once printed, cubes were checked visually to detect potential defects or foreign material (*e.g.*, leftover of a previous print on the 3D printer bed). No anomalies were detected. Before being used, they were stored in a clean, mild temperature and dim light room. Finally, one should note that detailed 3D printing materials composition were not available, as they are considered a trade secret, a common problem already encountered by other research teams (14, 21).

Runs were started on Friday. First, 500 mL of *Chlorella vulgaris* culture with an optical density of 0.03 (750 nm) was prepared and thoroughly mixed. Then, 50 ml were transferred into eight different flasks. Two flasks were supplemented with one cube, two others with two cubes, and another set of two with three cubes (all cubes made of the same material). The two remaining flasks were used as negative control (B3N medium and cells only) and positive control (B3N medium, cells, and potassium dichromate at 4 mg/L (32, 33)). Flasks were then installed in this incubator and monitored daily (except over the weekend).

2 3. Growth monitoring

Samples of 1 mL were withdrawn from the flasks daily. Cell development was followed using optical density (Shimadzu UV-1800 spectrophotometer) as a proxy of cells' dry weight. Samples with an optical density above 0.4 were diluted to fall below this value in order not to go over the linear portion of the calibration curve. The optical density was recorded at 750 nm. Indeed, this wavelength allows to account for cell walls and not pigments, hence measuring only for biomass (34). Furthermore, frequent microscope observations were done to check the cell condition (size, aggregation, color, presence of a large vacuole (35), ...) and potential contamination.

2 4. Flow cytometry assay

In parallel to biomass quantification, cell status was analyzed using flow cytometry (BD Fortessa x20). Four parameters were recorded: forward scatter (or FCS, blue laser at 488 nm) as a proxy of cell size, side scatter (or SSC, blue laser at 488 nm, 488/10 nm detection) as a proxy of cell complexity, chlorophyll fluorescence (blue laser at 488 nm, 695/40 nm detection), and cell reactive oxygen species content, by means of H_2DCFDA probing. H_2DCFDA is a molecule entering the cells before being cleaved by esterase and reacting with reactive oxygen species to release its fluorescent compound. Its use requires a specific procedure (36, 37). In short, fresh cells were incubated in the dark in the presence of 120 µM fresh H_2DCFDA (Sigma Chemicals, 200 µL dye, and 800 µL culture) for 15 minutes. Afterward, to remove the probe in excess, cells were pelleted (15000 rpm, 4 °C, 5 min), and the supernatant was discarded. The pellet was resuspended before immediate analysis. The dye signal was recovered using the blue laser (488 nm, 530/30 nm detection). In addition, positive control cells viability was assessed using propidium iodine. This molecule enters permeable, *i.e.* dead, cells and binds to their DNA, incidentally inducing its fluorescence upon excitation. To lead this assay, 990 µL of fresh cells were mixed with 10 µL of 1 g/L fresh propidium iodide (Sigma Chemicals). Afterward, cells were pelleted by centrifugation (15000 rpm, 4 °C, 5 min), and the supernatant was discarded to separate the cells from the probe remaining in suspension. The pellet was resuspended before immediate analysis. The dye signal was recovered using the yellow-green laser (561 nm, 610/20 nm detection). Finally, for all the aforementioned tests, at least 30 000 events were recorded per analysis.

2 5. Photosynthetic apparatus qualification - OJIP assays

At the end of the runs, fresh samples (*circa* 3 mL) were collected and placed in a dark enclosure for 15 minutes immediately after their withdrawal from the culture vessel. Afterwards, transient variable chlorophyll fluorescence assays (also referred to as OJIP tests) were carried out in order to evaluate photosynthetic apparatus status (AquaPen 110-C). First, the signals were checked for potential saturation (never encountered). Then, they were processed according to the recommendations of Strasser (38). From a qualitative perspective, the general dynamic of the fluorescence signal was analyzed (succession of OJIP stages). From a quantitative perspective, values relatives to the Reaction Centers (RC) were computed. The three primary parameters were: absorption per reaction center (ABS/RC), trapping per reaction center (TR_0/RC), and transfer per reaction (ET_0/RC). ABS/RC accounts for the quantity of energy captured by antennae associated with a reaction center. TR_0/RC focuses on the fraction of this energy that is directed toward the core of the photosystem II (PSII). Consequently, the dissipated amount of energy can be computed as ABS/RC - TR_0/RC. Finally, ET_0/RC relates to the amount of excitation leaving the PSII down the electron chain (towards the PQ pool, the cytochrome $b_{6/f}$, and the PSI).

2 6. Pigment extraction and quantification

Once the sample dedicated to the photosynthetic apparatus qualification had been withdrawn, the remaining biomass and the cubes were recovered. Cells were washed twice by centrifugation and resuspension in milliQ water (4 °C, 11000 rpm, 10 minutes). The pellet was then frozen and freeze-dried (1-day primary drying, 1-day secondary drying, Christ alpha 1-2 LD +). If not processed immediatly, the microalgae powder was stored in the dark at -20 °C before being used for pigment extraction. For the extraction, 1 mg of powder was
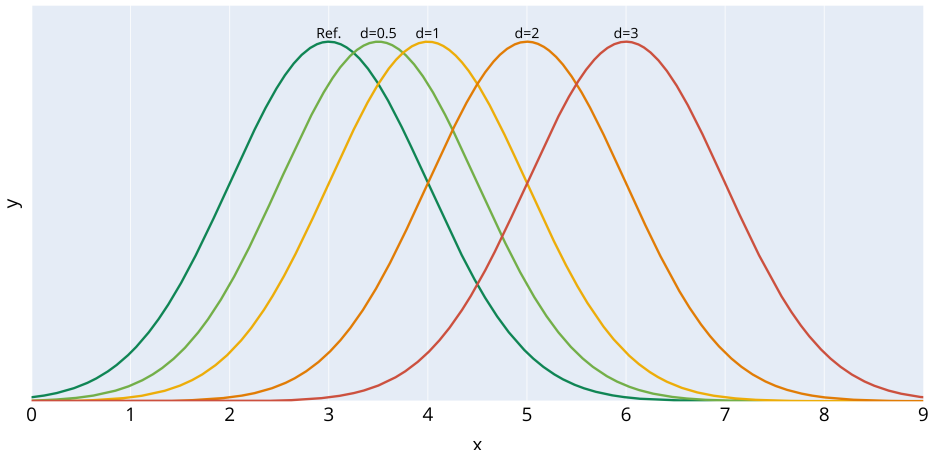
Fig. 1. Illustration of Gaussian curve overlap for different Cohen's d value. Standard deviation - 1, Reference curve mean - 3

homogenized in 5 ml pure methanol using MP Biomedicals FastPrep42 bead beater. Followinf Porra's advice for recalcitrant microalgae, such as *Chlorella vulgaris*, the suspension was cooked for 20 minutes at 60 °C (shaded from light) (39). Finally, after a cooling period, the extract wasfiltered (0.22 μm) and absorbance spectrum was recorded (Shimadzu UV-1800). The obtained spectra were processed with the help of Wellburn's equations for pure methanol and high precision spectrophometer (Eq. 1, 2 and 3). Ultimately, these equations allowed to compute chlorophyll *a*, chlorophyll *b* and total carotenoids (40) concentration.

$$Chl_a = 16.72\, A_{665.2nm} - 9.16\, A_{652.4nm} \qquad \text{(1)}$$

$$Chl_b = 34.09\, A_{652.4nm} - 15.28\, A_{665.2nm} \qquad \text{(2)}$$

$$Car_{x+c} = (1000\, A_{470nm} - 1.63\, Chl_a - 104.96\, Chl_b)/221 \qquad \text{(3)}$$

where $A_{665.2nm}$, $A_{652.4nm}$, and A_{470nm} are the recorded absorbance of the pigment extracts at the wavelengths specified as subscripts.

2 7. Recovered 3D printing material cubes observations

Recovered cubes were qualitatively inspected to assess if and to which extent microalgae would have colonized their surface. To do so, they were placed under a microscope (Zeiss Apotme 2, up to 168x magnification) mounted with fluorescence capabilities. In order to enhance the contract between the cells and the materials, the scenes were observed with a fluorescence setup (572/26 nm excitation and 645/90 nm emission) as it stimulates chlorophyll fluorescence. Therefore, *Chlorella vulgaris* cells appear as tiny glowing white dots on the pictures. In addition to cubes put in contact with microalgae, pristine cubes were also observed as control.

2 8. Statistical analysis

Statistical significance was assessed using the ANOVA test. When the null hypothesis was rejected ($p < 0.05$), data were further analyzed using Tukey's Honestly Significant Difference test. In terms of reporting, if not stated otherwise, the following results are presented as the mean of the replicate, while the error bars account for the spread. Indeed two tests are too few to draw meaningful standard deviations. For the same reason, in most figures, the two runs of the duplicate were drawn.

Another statistical tool was used to analyze flow cytometry readings. As all the populations exhibited a Gaussian shape, it was possible to resort to Cohen's d index to qualify how far away from each other they were. Using this index allows to report synthetic results without drawing each population (7 runs x 4 time-points x 4 monitored parameters, *i.e.*, 112 per tested materials) in overcrowded graphs. From a technical point of view, Cohen's d index is calculated by norming the difference of the means of two populations by their pooled standard deviation (Eq. 4) (41, 42). Figure 1 illustrates the span between different Gaussian curves for various Cohen's d index values. From the graph, one can draw a general rule of thumb for cytometry readings: $d < 0.5$ represents a small difference, $0.5 < d < 1$ a medium one, $1 < d < 2$ a significant one, with the two populations starting to detach from one another, and $d > 2$ a clear indicator of two different population.

$$d = \frac{\mu_1 - \mu_2}{\sqrt{\dfrac{(n_1 - 1)\sigma_1^2 + (n_2 - 1)\sigma_2^2}{n_1 + n_2}}} \qquad \text{(4)}$$

where d is Cohen's metric, μ_1 and μ_2 the mean values of the two populations tested, σ_1 and σ_2 the standard deviations of the two populations tested, and n_1 and n_2 the number of samples of the two populations tested.

3. Results and discussion

3 1. Cell proliferation

Figure 2 presents the evolution of the cultures' optical density at 750 nm (proxy of the cell concentration) over the duration of the experiments. As one can see, all the cultures exhibit an exponential trend followed by a slowdown around the experiments' last day, corresponding to the entry in the stationary phase. ABS, PC-Blend, and PLA materials showed growth profiles similar to negative controls (p-values of 0.244, 0.943,
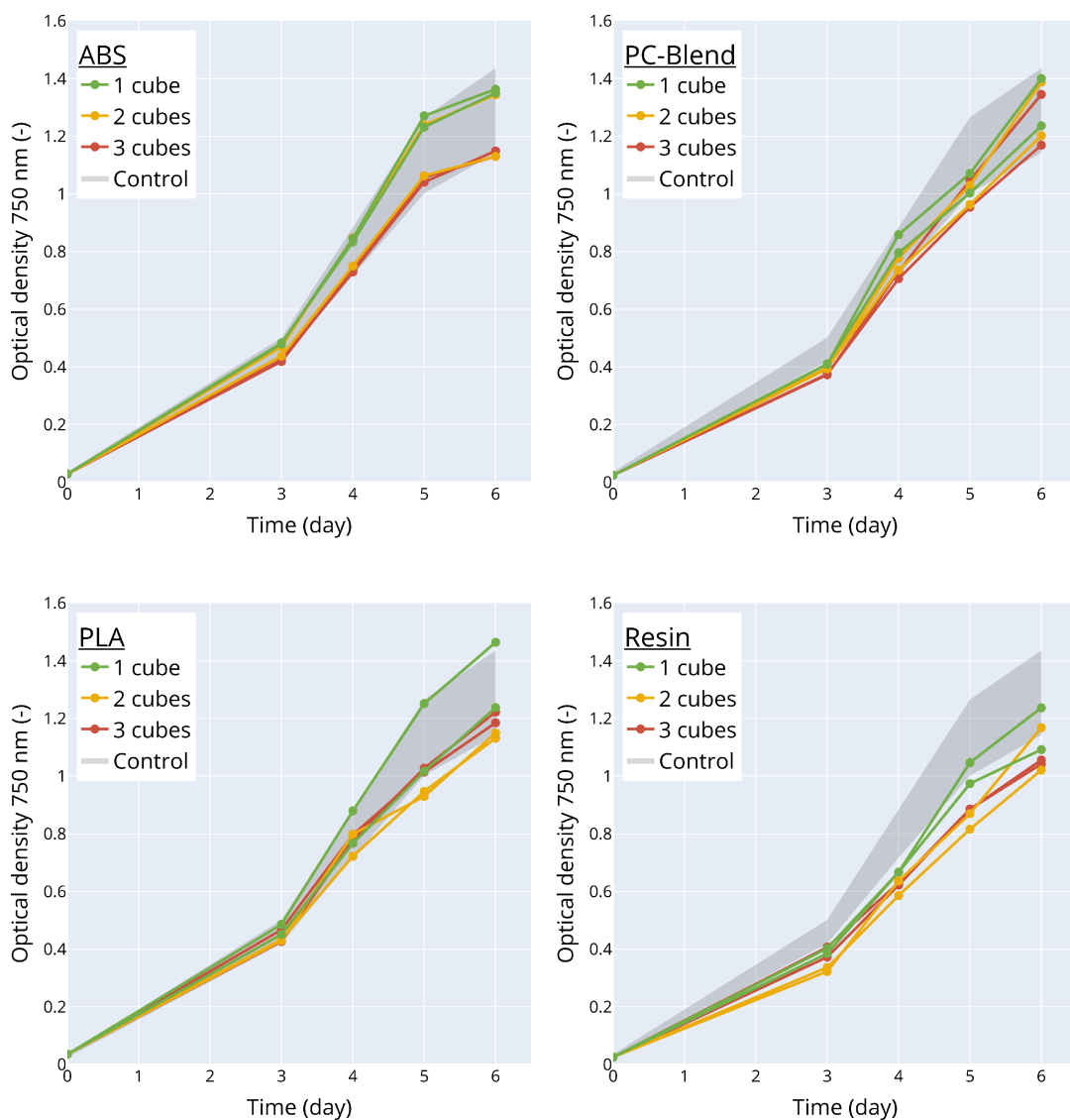
Fig. 2. Culture optical density at 750 nm over time for the four tested materials. When optical density was higher than 0.4 a dilution was applied. Shaded area - spread of all the control runs

and 0.233, respectively). The resin material offers a growth profile appearing below the controls. This observation can be deemed marginally significant (p = 0.059). Going further, it is the 3-cube runs that fall below the range of nominal performances (p = 0.077). This finding suggests the existence of a dose-response mechanism with this material, discussed hereinafter.

For all the runs, the positive control showed no sign of cell proliferation. The optical density kept stable around the inoculation value. Moreover, microscope examination revealed that the majority of the cells were bleached.

3 2. Cell status

Monitoring cell growth can only be the first step in evaluating the interactions between microalgae and 3D printing material. Indeed, while of prime interest, especially from a biotechnological point of view, its macroscopic nature would prevent it from detecting subtle cell-scale changes. With this view in mind, flow cytometry offers a potent tool to discrim-

inate these potential evolutions at the cell level. Flow cytometry analyses are reported in Figure 3 by means of Cohen's d indices. For all the time points, the negative control was taken as the reference. Therefore, the presented curves represent the standardized difference between a given configuration (material and number of cubes) and the associated control run.

First of all, a general comment is that cells' morphology (Forward SCatter, or FSC, as a proxy of size, and Side SCatter, or SSC, as a proxy of cytoplasmic complexity) did not exhibit much changes compared to control for most materials. Only ABS appears to transiently induce swelling of the cells, with a somewhat larger size and complexity on days four and five. The same comment can be drawn for all the materials regarding chlorophyll fluorescence signal. Indeed, none reached a Cohen's d value above 0.5. From these indicators, it can be concluded that the cells appear in the same conditions as the control, with similar size, internal morphology, and color.
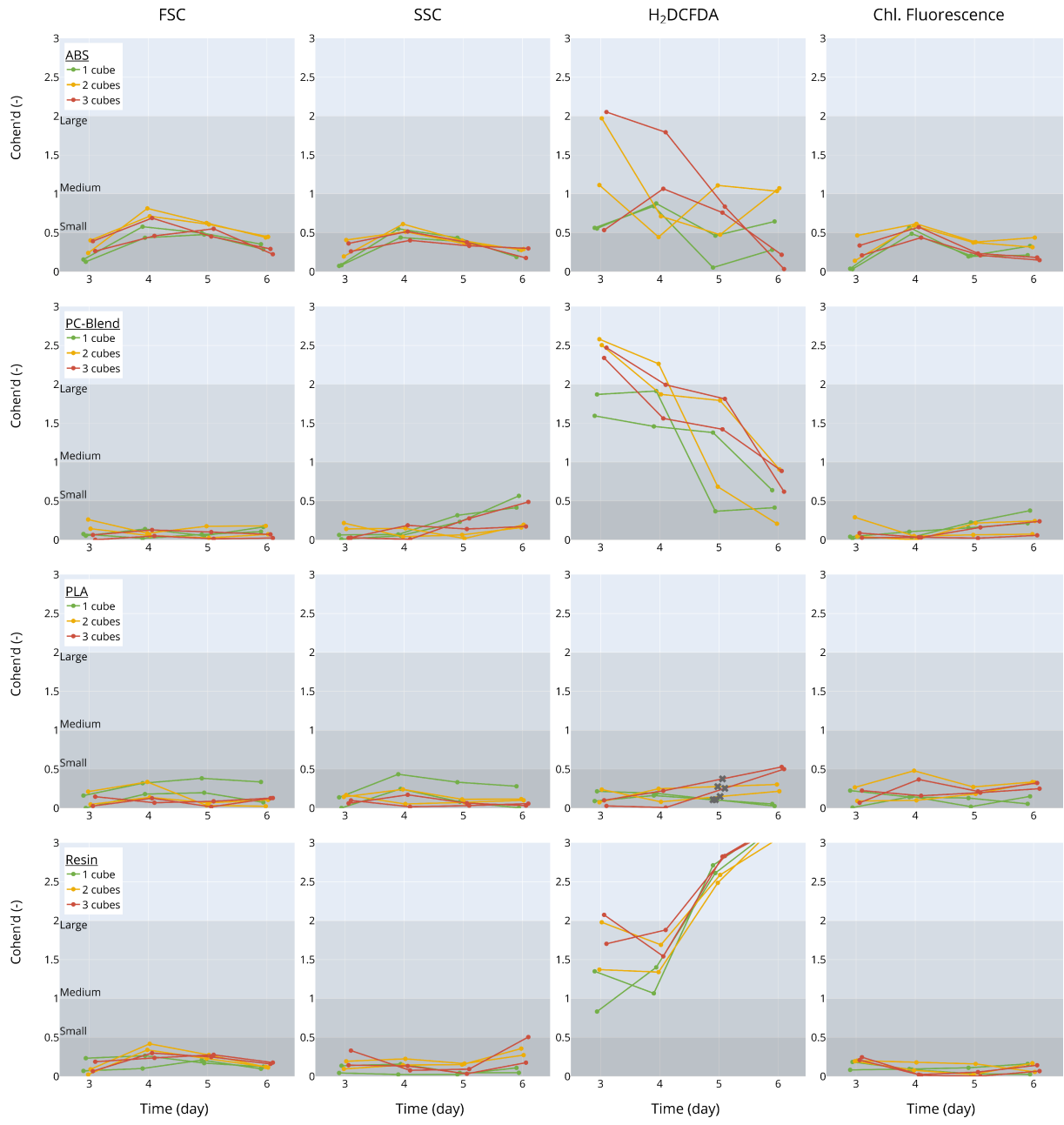
Fig. 3. Flow cytometry reading presented as standardized deviations to control (Cohen's d index, see Eq. 4). For PLA material on day five, the H_2DCFDA of the control run yielded abhorrent values. After checking that H_2DCFDA of the test configurations were within the range of the previous and the following days, it was decided to remove the computed indices and replace them with their linear interpolations, marked as crosses

Yet, H_2DCFDA modulates this purely observational conclusion. Indeed, reactive oxygen species probing shows that most of the materials actually induce an intercellular response. ABS and PC-Blend curves show a clear decreasing trend. It starts with a medium to large difference to control on day three, and decreases to a medium to small difference at the end of the run. The signal level also appears to be correlated with the number of cubes, suggesting a potential dose-response mechanism that attenuates in time. This trend may correspond to a progressive metabolizing of some substance initially released by the cubes. Indeed, plastic materials are not pure polymers. They are often supplemented by plasticizers (7 % in mass, on average)(43).

Those molecules (*e.g.*, dibutyl phthalate, bisphenol A, 3,3'-diaminobenzidine-like substances (44)) can be water soluble and enter in contact with microalgae cells. In the ecotoxicity community, they are commonly identified within plastic leachates, and their overall detrimental effects on microalgae are well-established, while the associated metabolic pathways are still unclear (45–47). Focusing on the 3D printing material/microalgae interaction, some authors deployed curation procedures to eliminate the leachates (14). In contrast, others did not (15, 17) without seeing detrimental effects, allegedly because they used PLA or medical-grade material. Another possibility could be the unknown compounds manufacturers use to improve their 3D printing materials proper-
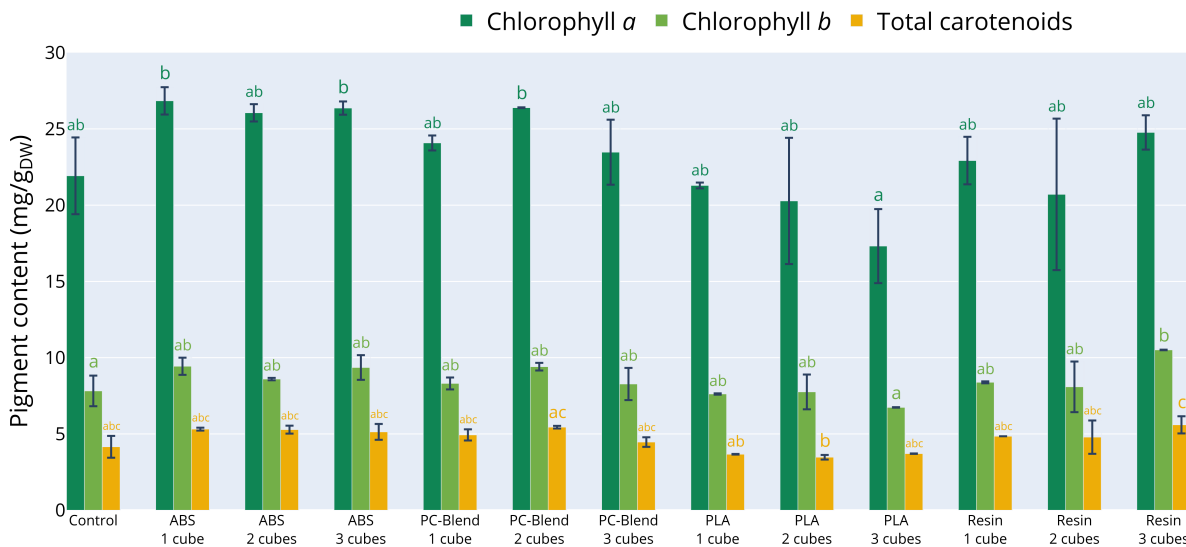
Fig. 4. Cell pigment content for the four tested materials, presented as mean and spread (error bars). One should note that positive controls are not reported as too little biomass was harvest which prevented to lead proper pigment profiling

ties ([14](#), [21](#)). Some might be harmful, while others not.

The case of the resin material is even more striking. The intracellular reactive oxygen species are detected at a large level on day three and start soaring continuously from day four. These observations lead to the conclusion that the resin material itself may be the origin of the problem. This conclusion is not surprising. Indeed, the cytotoxicity of such material was evidenced in the dental context ([48](#)). In their study, the authors exposed Hela cells to 23 monomers and tested viability in a dose-response approach. They concluded that the acrylates were more toxic than the corresponding methacrylates and that the longer the chain, the lower the IC_{50}. They relied on literature to hypothesize that molecules' lipophilicity helped them to cross the cell membrane and deploy their cytotoxic effects. Furthermore, tests on zebrafish showed that resin-printed parts could induce severe detrimental effects (preventing eggs from hatching and causing embryo deaths) ([21](#)). In this test, the authors also confirmed the presence of leachates in the culture medium for uncured resin material. While they did not analyze them for cured resin, they hypothesized that the improved performances of the UV-cured resin were linked to their reduction.

Finally, PLA is the only material that does induce a rise in intracellular reactive oxygen species levels, with a deviation kept at a low level.

3 3. Cell pigment content

Figure [4](#) illustrates the cell pigment contents for all the configurations. The first qualitative comment is that all the cultures present a similar pigment profile. Indeed, statistical analysis shows that the differences are mainly between samples, while most can be considered similar to control. From a quantitative perspective, the observed pigment profile can be deemed rich in chlorophyll *a* and *b* (23.2 ± 3.2 mg/g_{DW}, and 8.4 ± 1.1 mg/g_{DW}, respectively). Furthermore, total

carotenoid pigment levels are also quite stable (4.67 ± 0.79 mg/g_{DW}) with a ratio of total carotenoids over total chlorophyll of 0.15 ± 0.01. Taking a step back, these values correlate with previous studies with the same strain under a similar illumination ([49](#)), and echoes the original intention to supply non-limiting low illumination to exacerbate microalgae pigment expression. Furthermore, the fact that all the runs are relatively close to the control one suggests that the cell photosynthetic apparatus is not severely impaired. While interesting, especially from a biotechnological point of view for which pigments represent a subsequent part of the microalgae commercial value supporting the whole value chain, *in vivo* pigment profiling is incapable of detecting subtle alteration of photosynthesis functioning. Therefore, it is necessary to dive further and analyze the dynamic of the *in vivo* photosystems, which was accessed via OJIP tests.

3 4. Photosynthetic apparatus status

Table [1](#) reports the detailed photosynthetic apparatus status for all the runs. First, one can see that the positive control runs exhibit a severely impaired apparatus. The very high values of ABS/RC, TR_0/RC, and ET_0/RC suggest that a large fraction of the photosystems are damaged on both donor and acceptor sides. Then, ABS, PC-Blend, and PLA runs yield a behavior similar to control runs (p-values of 0.505, 0.378, and 0.293 for the three indicators, respectively). This observation tends to agree with the flow cytometer reading. Indeed, the amount of stress experienced by the microalgae is maximum at day three and decreases afterward. As the OJIP tests are led on the last day, cells were allowed enough time to cope with it and return to a nominal functioning, at least from a photosynthetic point of view.

On the contrary, the contact with resin material induced a negative alteration of the cell photosynthetic apparatus. It is characterized by a moderate, yet significant, increase

Run		ABS/RC	TR_0/RC	ET_0/RC
Negative control		1.66 ± 0.22	1.16 ± 0.07	0.48 ± 0.04
Positive control		5.32 ± 2.89	1.81 ± 0.67	0.54 ± 0.30
ABS	1 cube	1.63 ± 0.02	1.18 ± 0.02	0.50 ± 0.01
	2 cubes	1.55 ± 0.00	1.14 ± 0.00	0.48 ± 0.01
	3 cubes	1.53 ± 0.00	1.13 ± 0.01	0.49 ± 0.01
PC-Blend	1 cube	1.47 ± 0.04	1.09 ± 0.02	0.48 ± 0.00
	2 cubes	1.55 ± 0.09	1.12 ± 0.05	0.48 ± 0.01
	3 cubes	1.58 ± 0.00	1.14 ± 0.00	0.48 ± 0.00
PLA	1 cube	1.40 ± 0.15	1.13 ± 0.01	0.48 ± 0.01
	2 cubes	1.62 ± 0.07	1.16 ± 0.03	0.47 ± 0.00
	3 cubes	1.64 ± 0.01	1.15 ± 0.00	0.45 ± 0.01
Resin	1 cube	1.71 ± 0.08	1.23 ± 0.02	0.52 ± 0.02
	2 cubes	2.03 ± 0.01	1.40 ± 0.00	0.56 ± 0.00
	3 cubes	$1.93 \pm -$	$1.36 \pm -$	$0.56 \pm -$

Table 1. Indicator of the photosynthetic apparatus functioning drawn from OJIP test. Data of the duplicate run for resin material with three cubes were lost, hence the lack of spread

in ABS/RC, TR_0/RC, and ET_0/RC, with p-values of 0.010, 0.001, and 0.004, respectively. Here again, this observation aligns well with the flow cytometry readings and correlates the important , yet non lethal, level of stress undergone by the culture even at the end of the run.

3 5. Cubes observations

The study's final analysis was to examine the cubes that had been submerged for six days (for pictures, see supplementary material). The first qualitative comment is that the cubes' surfaces exhibit the expected surface condition: stacks of layers for ABS, PC-Blend, and PLA, mesh-like for the resin. This mesh-like surface comes from the pixels of the screen used in the 3D printer to realize the photopolymerization of the resin. Then, some artifacts are already present on virgin cubes. They appear as large white dots (especially in the case of PC-Blend). Nevertheless, one can discern the microalgae cells. They can be spotted as tiny white dots. For the three first materials, they are usually grouped in between the 3D printing materials layers, giving them the aspect of horizontal lines. For the resin, they form small, unevenly spread, and rare groups. For all materials, it can be concluded that microalgae did not alter the shape of the printed model, over the course of the cultivation.

As for any visual observation, the evaluation is mainly qualitative. Nevertheless, it is possible to assess a general trend: PLA is the material hosting the highest amount of cells, followed by ABS and PC-Blend. Finally, the resin surface did not seem to host many groups of cells. Even though qualitative, this observation is in good agreement with quantitative data obtained from the flow cytometry and fluorimetric assays.

These observations cannot help to assess for potential dose-response mechanisms. Indeed, as for OJIP tests, they were led at the end of the run, hence after a potential acclimation of microalgae to ABS and PC-Blend. Furthermore, regarding the possible colonization of biofilm, it was not evidenced in any configuration. Yet, the cultivation duration, one week, might have needed to be longer to highlight such

a phenomenon ([14], [15]).

4. Conclusion

Microalga *Chlorella vulgaris* was cultivated in contact with different 3D printing materials. Acrylate methacrylate resin material inhibits growth. ABS, PC-Blend, and PLA led to nominal growth, photosynthetic apparatus status, and colonization of the materials by the microalgae. PLA was the only material that did not induce an early onset of intracellular reactive oxygen species levels. Therefore, resin is to be ruled out as photobioreactor material, ABS and PC-Blend could be used after a curation period. Finally, this studies calls for a longer one studying 3D printing material aging when placed in contact with microalgae and their culture media.

E-supplementary data for this work can be found in e-version of this paper online.

Bibliography

1. Wendie Levasseur, Patrick Perré, and Victor Pozzobon. A review of high value-added molecules production by microalgae in light of the classification. *Biotechnology Advances*, 41:107545, July 2020. ISSN 0734-9750. .

2. Pau Loke Show. Global market and economic analysis of microalgae technology: Status and perspectives. *Bioresource Technology*, 357:127329, August 2022. ISSN 0960-8524. .

3. Said Abu-Ghosh, Dror Fixler, Zvy Dubinsky, and David Iluz. Flashing light in microalgae biotechnology. *Bioresource Technology*, 203:357–363, March 2016. ISSN 0960-8524. .

4. Peter S. C. Schulze, Celeste Brindley, José M. Fernández, Ralf Rautenberger, Hugo Pereira, René H. Wijffels, and Viswanath Kiron. Flashing light does not improve photosynthetic performance and growth of green microalgae. *Bioresource Technology Reports*, 9:100367, February 2020. ISSN 2589-014X. .

5. Imma Gifuni, Antonino Pollio, Antonio Marzocchella, and Giuseppe Olivieri. New ultra-flat photobioreactor for intensive microalgal production: The effect of light irradiance. *Algal Research*, 34:134–142, September 2018. ISSN 2211-9264. .

6. Victor Pozzobon. Chlorella vulgaris cultivation under super high light intensity: An application of the flashing light effect. *Algal Research*, 68:102874, November 2022. ISSN 2211-9264. .

7. Wendie Levasseur, Victor Pozzobon, and Patrick Perré. Green microalgae in intermittent light: a meta-analysis assisted by machine learning. *Journal of Applied Phycology*, October 2021. ISSN 1573-5176. .

8. Xi Gao, Bo Kong, and R. Dennis Vigil. Simulation of algal photobioreactors: recent developments and challenges. *Biotechnology Letters*, 40(9):1311–1327, October 2018. ISSN 1573-6776. .

9. Wenbiao Jiang, Wendie Levasseur, Joel Casalinho, Thierry Martin, François Puel, Patrick Perré, and Victor Pozzobon. Shear stress computation in a millimeter thin flat panel photobioreactor: Numerical design validated by experiments. *Biotechnology and Applied Biochemistry*, 68(1):60–70, 2021. ISSN 1470-8744. . _eprint: https://iubmb.onlinelibrary.wiley.com/doi/pdf/10.1002/bab.1894.

10. Iris Perner-Nochta and Clemens Posten. Simulations of light intensity variation in photobioreactors. *Journal of Biotechnology*, 131(3):276–285, September 2007. ISSN 0168-1656. .

11. Victor Pozzobon and Patrick Perré. Multiscale numerical workflow describing microalgae motion and light pattern incidence towards population growth in a photobioreactor. *Journal of Theoretical Biology*, 498:110293, August 2020. ISSN 0022-5193. .

12. Jianke Huang, Fei Feng, Minxi Wan, Jiangguo Ying, Yuanguang Li, Xiaoxing Qu, Ronghua Pan, Guomin Shen, and Wei Li. Improving performance of flat-plate photobioreactors by installation of novel internal mixers optimized with computational fluid dynamics. *Bioresource Technology*, 182:151–159, April 2015. ISSN 0960-8524. .

13. Cesar Parra-Cabrera, Clement Achille, Simon Kuhn, and Rob Ameloot. 3D printing in chemical engineering and catalytic technology: structured catalysts, mixers and reactors. *Chemical Society Reviews*, 47(1):209–230, 2018. . Publisher: Royal Society of Chemistry.

14. Matthew Ryley, Megan Carve, Richard Piola, Andrew J. Scardino, and Jeff Shimeta. Comparison of biofouling on 3D-printing materials in the marine environment. *International Biodeterioration & Biodegradation*, 164:105293, October 2021. ISSN 0964-8305. .

15. Young Joon Sung, Hong Ki Yoon, Jeong Seop Lee, Jaemin Joun, Byung Sun Yu, Ranjna Sirohi, and Sang Jun Sim. Novel 3D-printed buoyant structures for improvement in flue gas CO2-derived microalgal biomass production by enhancing anti-biofouling on vertical polymeric photobioreactor. *Journal of Cleaner Production*, 366:133030, September 2022. ISSN 0959-6526. .

16. Jeong Seop Lee, Young Joon Sung, and Sang Jun Sim. Kinetic analysis of microalgae cultivation utilizing 3D-printed real-time monitoring system reveals potential of biological CO2 conversion. *Bioresource Technology*, 364:128014, November 2022. ISSN 0960-8524. .

17. Maira Shakeel Syed, Mehdi Rafeie, Rita Henderson, Dries Vandamme, Mohsen Asadnia, and Majid Ebrahimi Warkiani. A 3D-printed mini-hydrocyclone for high throughput particle separation: application to primary harvesting of microalgae. *Lab on a Chip*, 17(14):2459–2469, July 2017. ISSN 1473-0189. . Publisher: The Royal Society of Chemistry.

18. Zaida Natalia Uribe-Wandurraga, Lu Zhang, Martijn W. J. Noort, Maarten A. I. Schutyser, Purificación García-Segovia, and Javier Martínez-Monzó. Printability and Physicochemical Properties of Microalgae-Enriched 3D-Printed Snacks. *Food and Bioprocess Technology*, 13(11):2029–2042, November 2020. ISSN 1935-5149. .

19. Zaida Natalia Uribe-Wandurraga, Marta Igual, Javier Reino-Moyón, Purificación García-Segovia, and Javier Martínez-Monzó. Effect of Microalgae (Arthrospira platensis and Chlorella vulgaris) Addition on 3D Printed Cookies. *Food Biophysics*, 16(1):27–39, March 2021. ISSN 1557-1866. .

20. Chaesu Kwak, Seoung Young Ryu, Hyunsu Park, Sehyeong Lim, Jeewon Yang, Jieun Kim, Jin Hyung Kim, and Joohyung Lee. A pickering emulsion stabilized by chlorella microalgae as an eco-friendly extrusion-based 3D printing ink processable under ambient conditions. *Journal of Colloid and Interface Science*, 582:81–89, January 2021. ISSN 0021-9797. .

21. Shirin Mesbah Oskui, Graciel Diamante, Chunyang Liao, Wei Shi, Jay Gan, Daniel Schlenk, and William H. Grover. Assessing and Reducing the Toxicity of 3D-Printed Parts. *Environmental Science & Technology Letters*, 3(1):1–6, January 2016. . Publisher: American Chemical Society.

22. Aurora Silva, Sónia A. Figueiredo, M. Goreti Sales, and Cristina Delerue-Matos. Ecotoxicity tests using the green algae Chlorella vulgaris—A useful tool in hazardous effluents management. *Journal of Hazardous Materials*, 167(1):179–185, August 2009. ISSN 0304-3894. .

23. Wendie Levasseur and Victor Pozzobon. Chapter 13 - Photosynthesis in bioremediation. In Junaid Ahmad Malik, editor, *Microbes and Microbial Biotechnology for Green Remediation*, pages 247–263. Elsevier, January 2022. ISBN 978-0-323-90452-0. .

24. Carl Safi, Bachar Zebib, Othmane Merah, Pierre-Yves Pontalier, and Carlos Vaca-Garcia. Morphology, composition, production, processing and applications of Chlorella vulgaris: A review. *Renewable and Sustainable Energy Reviews*, 35:265–278, July 2014. ISSN 1364-0321. .

25. Shih-Hsin Ho, Shu-Wen Huang, Chun-Yen Chen, Tomohisa Hasunuma, Akihiko Kondo, and Jo-Shu Chang. Characterization and optimization of carbohydrate production from an indigenous microalga Chlorella vulgaris FSP-E. *Bioresource Technology*, 135:157–165, May 2013. ISSN 0960-8524. .

26. Maja Šoštarič, Dušan Klinar, Mihael Bricelj, Janvit Golob, Marin Berovič, and Blaž Likozar. Growth, lipid extraction and thermal degradation of the microalga Chlorella vulgaris. *New Biotechnology*, 29(3):325–331, February 2012. ISSN 1871-6784. .

27. Hee-Jeong Choi. Parametric study of brewery wastewater effluent treatment using Chlorella vulgaris microalgae. *Environmental Engineering Research*, 21(4):401–408, August 2016. ISSN 1226-1025, 2005-968X. .

28. Alice Ferreira, Lusine Melkonyan, Sofia Carapinha, Belina Ribeiro, Daniel Figueiredo, Gayane Avetisova, and Luisa Gouveia. Biostimulant and biopesticide potential of microalgae growing in piggery wastewater. *Environmental Advances*, 4:100062, July 2021. ISSN 2666-7657. .

29. Waqas Muhammad Qazi, Simon Ballance, Katerina Kousoulaki, Anne Kjersti Uhlen, Dorinde M. M. Kleinegris, Kari Skjånes, and Anne Rieder. Protein Enrichment of Wheat Bread with Microalgae: Microchloropsis gaditana, Tetraselmis chui and Chlorella vulgaris. *Foods*, 10(12):3078, December 2021. . Number: 12 Publisher: Multidisciplinary Digital Publishing Institute.

30. Tina Eleršek, Karel Flisar, Blaž Likozar, Marina Klemenčič, Janvit Golob, Tadej Kotnik, and Damijan Miklavčič. Electroporation as a Solvent-Free Green Technique for Non-Destructive Extraction of Proteins and Lipids From Chlorella vulgaris. *Frontiers in Bioengineering and Biotechnology*, 8, 2020. ISSN 2296-4185.

31. Robert A. Andersen and Phycological Society of America. *Algal Culturing Techniques*. Academic Press, February 2005. ISBN 978-0-12-088426-1. Google-Books-ID: 9NADUHyFZaEC.

32. Jana Kvíderová. Rapid algal toxicity assay using variable chlorophyll fluorescence for Chlorella kessleri (chlorophyta). *Environmental Toxicology*, 25(6):554–563, 2010. ISSN 1522-7278. . _eprint: https://onlinelibrary.wiley.com/doi/pdf/10.1002/tox.20516.

33. V. A. Polynov, E. N. Maksimova, A. P. Safronov, and G. V. Kurlyandskaya. Influense of various forms of iron on growth of Chlorella vulgaris Beijer culture. *Journal of Physics: Conference Series*, 1389(1):012073, November 2019. ISSN 1742-6596. . Publisher: IOP Publishing.

34. Melinda J. Griffiths, Clive Garcin, Robert P. van Hille, and Susan T. L. Harrison. Interference by pigment in the estimation of microalgal biomass concentration by optical density. *Journal of Microbiological Methods*, 85(2):119–123, May 2011. ISSN 0167-7012. .

35. Hiroyuki Ishida, Masanori Izumi, Shinya Wada, and Amane Makino. Roles of autophagy in chloroplast recycling. *Biochimica et Biophysica Acta (BBA) - Bioenergetics*, 1837(4):512–521, April 2014. ISSN 0005-2728. .

36. Victor Pozzobon, Wendie Levasseur, Elise Viau, Emilie Michiels, Tiphaine Clément, and Patrick Perré. Machine learning processing of microalgae flow cytometry readings: illustrated with Chlorella vulgaris viability assays. *Journal of Applied Phycology*, 32(5):2967–2976, October 2020. ISSN 1573-5176. .

37. Na Cui, Patrick Perré, Emilie Michiels, and Victor Pozzobon. A Novel Strategy to Enhance Antioxidant Content in Saccharomyces Cerevisiae Based on Oxygen Pressure. *Bioengineering*, 10(2):246, February 2023. ISSN 2306-5354. . Number: 2 Publisher: Multidisciplinary Digital Publishing Institute.

38. Reto Jörg Strasser, Alaka Srivastava, and M. Tsimilli-Michael. The fluorescence transient as a tool to characterize and screen photosynthetic samples. *Probing photosynthesis: mechanisms, regulation and adaptation*, pages 445–483, 2000.

39. Robert J. Porra. A simple method for extracting chlorophylls from the recalcitrant alga, Nannochloris atomus, without formation of spectroscopically-different magnesium-rhodochlorin derivatives. *Biochimica et Biophysica Acta (BBA) - Bioenergetics*, 1019(2):137–141, August 1990. ISSN 0005-2728. .

40. Alan R. Wellburn. The Spectral Determination of Chlorophylls a and b, as well as Total Carotenoids, Using Various Solvents with Spectrophotometers of Different Resolution. *Journal of Plant Physiology*, 144(3):307–313, September 1994. ISSN 0176-1617. .

41. Gail M. Sullivan and Richard Feinn. Using Effect Size—or Why the P Value Is Not Enough. *Journal of Graduate Medical Education*, 4(3):279–282, September 2012. ISSN 1949-8349. .

42. Dongsheng Yang and Jarrod E. Dalton. A unified approach to measuring the effect size between two groups using SAS. In *SAS global forum*, volume 335, pages 1–6. Citeseer, 2012.

43. Roland Geyer, Jenna R. Jambeck, and Kara Lavender Law. Production, use, and fate of all plastics ever made. *Science Advances*, 3(7):e1700782, July 2017. ISSN 2375-2548. . Publisher: American Association for the Advancement of Science Section: Research Article.

44. Chunfeng Song, Zhengzheng Liu, Chenlin Wang, Shuhong Li, and Yutaka Kitamura. Different interaction performance between microplastics and microalgae: The bio-elimination potential of Chlorella sp. L38 and Phaeodactylum tricornutum MASCC-0025. *Science of The Total Environment*, 723:138146, June 2020. ISSN 0048-9697. .

45. Hongwei Luo, Yahui Xiang, Dongqin He, Yu Li, Yaoyao Zhao, Shuo Wang, and Xiangliang Pan. Leaching behavior of fluorescent additives from microplastics and the toxicity of leachate to Chlorella vulgaris. *Science of The Total Environment*, 678:1–9, August 2019. ISSN 0048-9697. .

46. Layla J. Hazeem, Gamze Yesilay, Mohamed Bououdina, Simone Perna, Demet Cetin, Zekiye Suludere, Alexandre Barras, and Rabah Boukherroub. Investigation of the toxic effects of different polystyrene micro-and nanoplastics on microalgae Chlorella vulgaris by analysis of cell viability, pigment content, oxidative stress and ultrastructural changes. *Marine Pollution Bulletin*, 156:111278, July 2020. ISSN 0025-326X. .

47. Shuangxi Li, Panpan Wang, Chao Zhang, Xiangjun Zhou, Zhihong Yin, Tianyi Hu, Dan Hu, Chenchen Liu, and Liandong Zhu. Influence of polystyrene microplastics on the growth, photosynthetic efficiency and aggregation of freshwater microalgae Chlamydomonas reinhardtii. *Science of The Total Environment*, 714:136767, April 2020. ISSN 0048-9697. .

48. Eiichi Yoshii. Cytotoxic effects of acrylates and methacrylates: Relationships of monomer structures and cytotoxicity. *Journal of Biomedical Materials Research*, 37(4):517–524, 1997. ISSN 1097-4636. . _eprint: https://onlinelibrary.wiley.com/doi/pdf/10.1002/%28SICI%291097-4636%2819971215%2937%3A4%3C517%3A%3AAID-JBM10%3E3.0.CO%3B2-5.

49. Victor Pozzobon, Na Cui, Alissa Moreaud, Emilie Michiels, and Wendie Levasseur. Nitrate and nitrite as mixed source of nitrogen for Chlorella vulgaris: Growth, nitrogen uptake and pigment contents. *Bioresource Technology*, page 124995, March 2021. ISSN 0960-8524. .